Validation of Gamma Probe Detection of the Sentinel Node in Melanoma

B.A.E. Kapteijn, O.E. Nieweg, S.H. Muller, I.H. Liem, C.A. Hoefnagel, E.J.Th. Rutgers and B.B.R. Kroon
Department of Surgery and Department of Nuclear Medicine, The Netherlands Cancer Institute, Amsterdam, The Netherlands

In melanoma, the presence or absence of metastasis in the first lymph node (sentinel node, SN) has a predictive value for the entire lymph node basin. This study explores the efficacy of lymphoscintigraphy with ^{99m}Tc-nanocolloid and a gamma-ray detection probe in tracing SNs. **Methods:** Sixty patients with clinically localized melanoma were studied. Lymphoscintigraphy was performed after intradermal injection of 60 MBq ^{99m}Tc-nanocolloid at the primary tumor site. Scintigraphy included early dynamic images and a body scan 2 hr postinjection. The following day, a gamma detection probe (Neoprobe® 1000) was used intraoperatively to trace the still radioactive SNs. The number of counts of the nodes and the surrounding tissues was measured before, during and after excision. Excised nodes and normal tissue samples were measured in a gamma well counter. The uptake of ^{99m}Tc-nanocolloid was calculated. **Results:** Lymphoscintigraphy showed 122 SNs distributed over 73 drainage basins. Use of the probe led to retrieval of all nodes that were searched for. The SN-to-background ratios were high: a median of 36 in vivo (range: 2–722) and a median of 274 ex vivo (range: 6–2,985). Counts in vivo correlated well with counts ex vivo. The mean percentage of the injected dose per SN was 0.69 (range: 0.0013–6.82), versus 0.23 (range 0.0004–2.59) in 23 measured second-echelon nodes (non-SNs). Mean percentage of uptake per gram tissue in SNs was 2.1 (range: 0.003-17.4), in skin 0.01 (range: 0.00–0.22) and in subcutaneous fat 0.0035 (range: 0.00–0.081). **Conclusion:** Average uptake of ^{99m}Tc-nanocolloid in SNs is substantially higher than uptake in non-SNs, skin and subcutaneous fat. The resulting high SN-to-background ratios facilitate the intraoperative detection of these nodes using a gamma detection probe.

Key Words: melanoma; sentinel node; lymphoscintigraphy; gamma probe; technetium-99m aggregated albumin

J Nucl Med 1997; 38:362–366

Ninety percent of patients with primary melanoma present without clinical evidence of metastases (*1*). Still, 20% of these patients harbor occult lymph node metastases presenting the surgeon with a dilemma (*2,3*). Prophylactic lymph node dissection results in a 50% survival rate when micrometastases are found, but means overtreatment of the other 80%, with a substantial morbidity (*4–7*). On the other hand, a wait and see policy results in a lower survival rate (20%–30%) when patients present with palpable metastasis during follow-up (*8–11*). Prospective and retrospective studies on this subject have shown conflicting results (*12–17*). The value of prophylactic lymph node dissection, therefore, remains a major controversy in the treatment of melanoma (*18*). New randomized studies by the American Cooperative Group and the World Health Organization Melanoma Program (*15*) may resolve this issue.

Morton et al. (*19*) have introduced a third approach. They developed a new method to identify clinically occult lymph node metastases in patients with melanoma. They hypothesized that a primary melanoma drains initially to a single lymph node, the so-called first-echelon or sentinel node (SN). The presence or absence of tumor in the SN is of predictive value for the status of the other lymph nodes in the regional basin. Several studies have proven this concept to be valid (*19–21*): the SN is indeed the first one to be involved when dissemination occurs. Morton et al. (*19*) initially used a nonradioactive dye to trace SNs. The sensitivity of this technique was approximately 80%. Lately, lymphoscintigraphy and gamma probe detection of radioactive tracers such as ^{99m}Tc-colloid and ^{99m}Tc-HSA have been suggested to increase the percentage of SNs that can be identified (*22,23*).

This study further explored the role of nuclear medicine to accurately identify SNs. The uptake of ^{99m}Tc-nanocolloid in SNs and surrounding normal tissues was investigated as well as the role of lymphoscintigraphy and a gamma detection probe to facilitate the surgical procedure.

MATERIALS AND METHODS

Patient Population

From December 1993 to January 1995, 60 consecutive patients (26 men, 34 women, age range 16–76 yr, mean age of 47 yr) with clinically localized melanoma were studied. The site of the melanoma was the leg (*30*), trunk (*16*), arm (*8*) and head/neck (*6*). Thirty-four patients had a superficial spreading melanoma, 22 nodular melanoma, 2 acrolentiginous melanoma, 1 lentigo maligna melanoma and in 1 patient the lesion could not be classified. The mean Breslow thickness of the tumors was 2.4 mm (range 1.1–8 mm). In 53 patients, the Breslow thickness was less than 4.0 mm. Ulceration was present in 17 lesions. Twelve patients had undergone wide excision with a margin range of 1–3 cm before lymphatic mapping.

Imaging

Patients were entered according to the criteria in Table 1. The day before surgery, all patients had lymphoscintigraphy to locate the SN. A mean dose of 57.8 MBq (range 26–79.2) Technetium-99m-nanocolloid in a volume ranging from 0.2–0.5 ml was injected with a 27-gauge needle adjacent to the biopsy wound or primary lesion when still present. The tracer was administered intradermally at two to eight points, depending on the length of the wound. Images were obtained using a dual-head gamma camera with low-energy, high-resolution collimators. Dynamic acquisition of 60 frames of 20 sec in a matrix of 128 × 128 × 1286 was started immediately to visualize the progress of lymphatic flow. If necessary, acquisition was continued for 45 min to adequately visualize the SN. Subsequently, anterior and lateral static images with an acquisition time of 300 sec in a 256 × 256 × 2566 matrix were obtained. To facilitate orientation, a ^{57}Co flood source with the 122-keV photon-energy peak was used for simultaneous transmission imaging. In addition to the standard anterior and lateral images, oblique views of 30–45° were obtained whenever the site of injection obscured the SN. Static images were repeated at 2 hr and, when nodes were not clearly depicted, at 4 hr after injection. SNs (first-echelon nodes) were defined as receiving drainage directly from the injection site. Non-SNs (second-echelon nodes)

Received Mar. 5, 1996; revision accepted Jul. 1, 1996.
For correspondence or reprints contact: B.A.E. Kapteijn, MD, The Netherlands Cancer Institute, Antoni van Leeuwenhoek Huis, Plesmanlaan 121, 1066 CX Amsterdam, The Netherlands.

TABLE 1
Criteria for Lymphatic Mapping and Sentinel Node Biopsy

Histologically-proven primary melanoma
Melanoma preferably excised with a small (2-mm) margin
No skin graft
Excision less than 3 mo previously
Breslow thickness 1 mm or more
No pregnancy

receive drainage from the SNs. Scintigraphy was used to determine the draining lymph node basin, to distinguish SNs from non-SNs, to determine the number of SNs and to mark their location on the skin with a dye.

Surgery

Surgery was performed on the day after scintigraphy. Just before the operation, patent blue dye (0.5–1.0 ml) was injected intradermally around the primary lesion or biopsy wound. Before incision, the accuracy of the skin mark was verified with a gamma detection probe (Neoprobe® 1000, Columbus, OH). The number of counts was also measured at another site within the same lymph node basin to establish a background value.

The site for the incision was chosen on the basis of the probe measurements. A small incision of a few centimeters was made. Blue-stained lymphatic channels were searched for in the subcutaneous tissue and dissected to the point where they drained into a blue lymph node. In the absence of blue discoloration, SNs were traced with the gamma probe on the basis of scintigraphy. The gamma probe was then used to measure the number of counts per second in the SN. An intraoperative background was measured in the open wound. The counting rate of the SN was also measured after excision (ex vivo). For an ex vivo background, the instrument table of the scrub nurse was used. Finally, the wound was scanned with the probe for SNs that might have been overlooked, due to limited resolution of lymphoscintigraphy. Non-SNs that were within easy reach were removed at the discretion of the operating surgeon.

Determination of Absolute Uptake

After the operation, all excised nodes (SN and non-SN) as well as small samples of skin and subcutaneous fat were measured in a gamma well counter and compared to a 10-kBq solution of ^{99m}Tc. The uptake of ^{99m}Tc-nanocolloid as a percentage of the injected dose per gram tissue and per node was calculated, with a correction for physical decay. After absolute uptake of radioactivity had been determined in the gamma well counter, all nodes were submitted for pathologic examination. A complete lymph node basin dissection was done when micrometastases were present.

RESULTS

Lymphatic transport of ^{99m}Tc-colloid starts immediately after administration of the agent. An SN could often be identified on the dynamic images within a few minutes. Non-SNs were visualized in the groin in the majority of cases, whereas in the axilla SNs were usually the only nodes depicted. In the groin, an average of 1.8 SNs (range 1–3) were visualized and in the axilla an average of 1.6 SNs (range: 1–3). In general, the images were easy to interpret (Fig. 1). Lymph channels were depicted in 48 of 60 patients. Dynamic imaging did not provide additional information in the remaining 12 patients. In six of these 12 patients this did not present us with a problem as only one node was visualized. At 2 hr after administration of ^{99m}Tc-nanocolloid, the lymphatic channels were usually no longer visible and the final node pattern was depicted. In nine patients, scans after 4 hr were needed because uncertainty existed whether hot spots were in fact remnant activity in the drainage ducts or no SN had

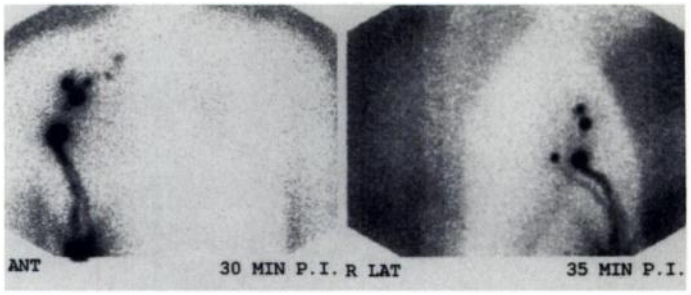

FIGURE 1. Lymphoscintigram of a 56-yr-old man with a melanoma on the right trunk. (A) The anterior images show lymphatic drainage to a sentinel node in the right axilla. (B) On the lateral images, another sentinel node with a separate drainage duct is visible.

as yet been visualized. Scintigraphy showed that most of the radioactivity remains at the injection site. Occasionally, the liver and the bladder were vaguely outlined.

Scintigraphy showed a total of 122 SNs in 73 lymph node basins in 59 of the 60 patients. Scintigraphy of one patient with a melanoma in the neck failed to show an SN, presumably due to proximity of the injection site. Forty-six patients had drainage to only one basin, 12 patients had SNs in two basins and one patient had SNs in three basins. Of the 13 melanomas with drainage to multiple basins, 12 were situated on the trunk and one on the scalp. Forty-one basins contained one SN, 16 contained two, 15 contained three and one basin contained four SNs.

Drainage to lymph nodes in unusual sites occurred in two patients: mediastinum and retroperitoneum. Lymphoscintigraphy of the 12 patients with previous wide excision showed no differences when compared to the other patients.

All SNs could be readily marked on the skin except in the three patients with an injection site adjacent to the lymphatic bed. Skin marks were found to be highly accurate in the groin and less so in other basins.

A total of 122 SNs was surgically removed. Five SNs were not removed: three were situated in the parotid gland, one in the mediastinum and one in the retroperitoneum. Exploration of these sites was considered to be excessive for an investigational procedure. The mean time between scintigraphy and surgery was 22 hr and 48 min (range 19.04–28.38).

Preoperative probe measurements on the operating table were performed in 52 patients and were successful in locating the SNs in 51 of them. In one patient, radiation from the nearby site of injection interfered with probe measurements. The surgeons found these preoperative measurements invariably helpful to choose the site for the incision. The median of the preoperative SN-to-background ratios was 13.9 (range 0–256).

Intraoperatively, 96 SNs were identified tracing blue-stained lymphatic channels. Probe measurements before excision showed that all these nodes were radioactive. Twenty-five nodes could not be identified with the blue dye, but these nodes were all identified with the probe. One node was located with blue dye at the site suggested by scintigraphy. Surprisingly, this node was not radioactive on the day of surgery. All nodes were retrieved from the same location as seen scintigraphically. Five SNs, not identified as such on the scans, were encountered intraoperatively by means of the blue dye and removed. The distribution of radioactivity over larger nodes could be determined with the probe. The counting rate was highest where the afferent blue lymphatic vessel entered the lymph node.

The median of the in vivo background measurements in the open wound was 28 cps (range: 5–520 cps). For the background ex vivo the median was 2.3 cps (range 0.5–17 cps). The probe

TABLE 2
Intraoperative and Ex Vivo Probe Measurements (cps) and Node-to-Background Ratios

Lymph nodes	n	cps		Node-to-background ratio	
		Range	Median	Range	Median
SN in vivo	121	47–12,982	1183	2–722	36
SN ex vivo	120	44–14,023	1165	6–2,985	274
Non-SN in vivo	9	15–2600	269	3–153	14.2
Non-SN ex vivo	23	3–2637	114	1–1,543	10.8
Wound bed after excision		5–540	47		

TABLE 3
Uptake of Technetium-99m-Nanocolloid in Sentinel Nodes

Sentinel node (n = 116)	Range	Median
Percent per node	1.3×10^{-3}–6.82	0.36
Percent per g node tissue	3×10^{-3}–17.4	1.0
MBq injected node	4×10^{-5}–0.25	0.0133
Blue-stained sentinel nodes (n = 92)		
Percent per node	1.3×10^{-3}–6.82	0.402
Percent per g node tissue	3×10^{-3}–17.4	1.09
MBq injected node	4×10^{-5}–0.25	0.0148
Unstained sentinel nodes (n = 24)		
Percent per node	2.6×10^{-3}–2.27	0.19
Percent per g node tissue	4.3×10^{-3}–9.6	0.69
MBq injected node	2×10^{-4}–0.16	0.0053

measurements of SNs both in vivo and ex vivo were much higher (Table 2). Ex vivo probe measurements were similar to the intraoperative measurements. A good correlation between in vivo and ex vivo measurements was found (Fig. 2).

In addition to the one node that was not radioactive, five nodes were not available for measurement in the well counter. In the remaining 116 nodes, uptake of ^{99m}Tc-nanocolloid per gram of tissue and per node were calculated and these data are presented in Table 3. When restricted to nodes that were not in part lost to frozen section microscopy, blue nodes had a significantly higher uptake of ^{99m}Tc-nanocolloid than unstained nodes (Wilcoxon rank-sum test, $p = 0.032$). For this set of nodes there was also a good correlation between the uptake and the in vivo counting rates (Fig. 3).

Twenty-three non-SNs were removed and available for well counter measurements. Seven of these nodes were blue, 16 were found with the probe. Uptake in these nodes was clearly lower than in the SNs (Table 4).

Lymph nodes are covered by skin and surrounded by fat. Uptake in these surrounding tissues was far less than in SNs. The average uptake of radioactivity in skin was 0.01%/g (range 0.0–0.22). For fat, the average uptake was 0.0035%/g (range 0.0–0.081).

Metastatic disease was found in 14 nodes in 10 patients (16.6%). Two patients with a tumor-free SN presented with metastasis in the same lymphatic bed during follow-up. The mean follow-up for our group of patients was 13.8 mo (range 8–21 mo).

DISCUSSION

This study documents the tissue distribution of ^{99m}Tc-nanocolloid and confirms the findings of others that scintigraphy and use of a gamma detection probe combined with patent blue dye can identify almost 100% of SNs in patients with melanoma (*24–26*).

Scintigraphy serves several purposes. Dynamic and static imaging are essential to indicate the drainage basin, determine the number of SNs, locate SNs outside the usual nodal basins (*21,27*) and differentiate SNs (first-echelon nodes) from non-SNs (second-echelon nodes). Dynamic imaging is especially useful as it can outline the drainage pattern. Static images after 30 min may not show the definitive status of the SN pattern. However, in most cases the pattern remains unchanged after 2 and 4 hr. The use of a flood source to outline the body contour is helpful for orientation (*28*).

Due to the limited resolution of the gamma camera, it is sometimes difficult to differentiate SNs from non-SNs and to determine the number of SNs when they are lying close to each other. The fact that we excised more lymph nodes than were shown on the images illustrates this point. Limited resolution or limited reproducibility of scintigraphy (*29,30*) could account for the two false-negative SNs. Repeat examination of the pathology specimens confirmed the absence of tumor in the removed SNs, ruling out the possibility of a histopathologic error.

The well counter measurements allow calculation of the absolute uptake of radioactivity in the nodes. Apart from the four SNs in two patients with unexplained deviant measurements, these data prove that the counting rates as measured intraoperatively with the probe accurately reflect the uptake of the tracer (Fig. 3). The good correlation (Fig. 2) between in vivo

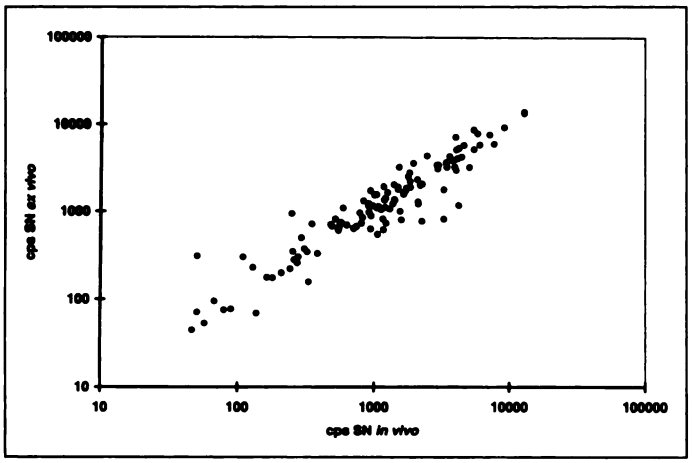

FIGURE 2. Correlation of sentinel node in vivo and ex vivo counting rates (coefficient = 0.94).

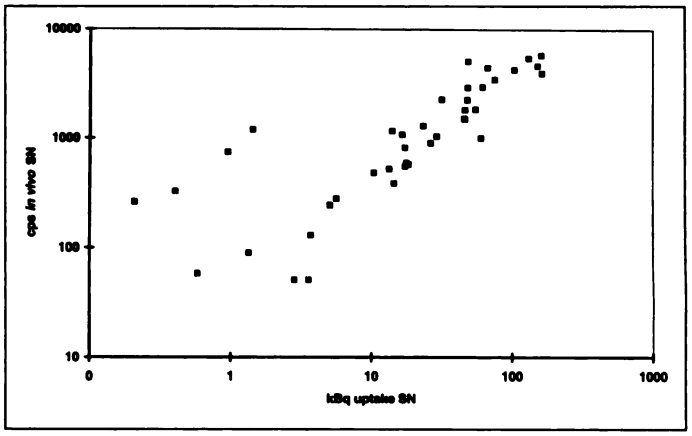

FIGURE 3. Correlation of ^{99m}Tc-nanocolloid uptake in the sentinel node with the counting rate measured in the wound.

TABLE 4
Uptake of Technetium-99m-Nanocolloid in Nonsentinel Nodes

Nonsentinel nodes (n = 23)	Range	Median
% per node	4.4×10^{-4}–2.59	0.02
% per g node tissue	1.5×10^{-4}–0.399	0.012
MBq injected node	1×10^{-5}–0.0185	4.3×10^{-4}

and ex vivo counting rates also indicates that the intraoperative probe measurements are indeed accurate and are not distorted by background, injection site or surrounding nodes. The well counter data also document the persisting high accumulation of ^{99m}Tc-nanocolloid in the SN compared to the surrounding normal tissues 23 hr after administration of the tracer.

The counting rate of the SNs was higher than the counting rate in the non-SNs (Tables 3 and 4). The first node in line appears to clear most of the radioactivity (*31*). Counting rates in this study are higher than those reported by other authors. Compared to our injected dose of approximately 60 MBq (1.6 mCi) 20 hr before surgery, Alex et al. report injection of 14.8 MBq (0.4 mCi) of ^{99m}Tc-sulfur colloid 2.5–5 hr before surgery (*32*). The counting rate that we found was higher, despite the fact that a smaller amount of radioactivity remained at the time of surgery, when corrected for decay. This observation may be due to a difference in kinetics between the two tracers. Approximately 77% of the ^{99m}Tc-nanocolloid has a particle size of 30 nm or less (*33,34*). Technetium-99m-nanocolloid has been reported to show a greater migration speed and a higher total activity over the visualized lymph nodes than other tracers such as ^{99m}Tc-antimony sulfide colloid, ^{99m}Tc-stannous sulfate, ^{99m}Tc-sulfur colloid, ^{99m}Tc-sulfur microcolloid and ^{99m}Tc-rhenium sulfur colloid (*30,34–36*). Also, there may exist a difference in sensitivity between different types of probes used by various investigators. The high SN-to-background ratios enable the tracing of the radioactive nodes from the time before the incision is made. The optimal advantage of these high ratios is obtained by using the probe in the static situation, when the radioactivity has cleared the lymphatic channels. A disadvantage of the probe in the static situation may become apparent when multiple nodes are depicted on the images. With this device, first-echelon nodes (SNs) cannot be distinguished from second-echelon nodes (non-SNs) because afferent and efferent lymphatic channels are not identified in the static situation. First-echelon nodes must be identified and marked based on dynamic scintigraphy beforehand.

Another approach is administration of a radioactive tracer on the operating table (*25,26*). With dynamic use of the probe, one can track the progression of the tracer through a lymphatic channel. Also, a smaller tracer dose is sufficient in this situation. However, dynamic use of the probe also has its drawbacks. SN-to-background ratios are not as high, because the accumulation in the node is still in its early phase and the radioactivity level of the background is relatively high. Tracking multiple lymphatic channels simultaneously may also present a problem. Finally, dynamic use of the probe requires the administration of the radiopharmaceutical in the operating room and handling of radioactivity outside the nuclear medicine department may be prohibited by local regulations.

We prefer to use the probe in the static situation and to use blue dye as an additional dynamic agent to resolve ambiguities in differentiating SNs from non-SNs.

CONCLUSION

This study shows that the uptake of ^{99m}Tc-nanocolloid in SNs is substantially higher than in nonsentinel nodes. Absolute uptake in the surrounding tissues (skin, subcutaneous fat) is extremely low. A good correlation exists between the uptake of ^{99m}Tc-nanocolloid in the SN and the counts measured with the probe. These features enable surgeons to reliably locate SNs intraoperatively through a small incision.

REFERENCES

1. Balch CM, Soong SJ, Shaw HM, et al. Changing trends in the clinical and pathologic features of melanoma. In: Balch CM, Houghton AN, Milton GW, Sober AJ, Soong SJ, eds. *Cutaneous melanoma*, 2nd ed. Philadelphia, PA: J.B. Lippincott Co.; 1992:40–45.
2. McNeer G, Das Gupta TK. Prognosis in malignant melanoma. *Surgery* 1964;56:512–518.
3. Karakousis CP, Emrich LJ, Rao U. Groin dissection in malignant melanoma. *Am J Surg* 1986;152:491–495.
4. Urist MM, Maddox WA, Kennedy JE, Balch CM. Patient risk factors and surgical morbidity after regional lymphadenectomy in 204 melanoma patients. *Cancer* 1983; 51:2152–2156.
5. Ames FC, Singletary SE. Cutaneous malignancies of the trunk and lower extremities. In: Johnson DE, Ames FC, eds. *Groin dissection*. Chicago, IL: Year Book Medical Publishers Inc.; 1985:111–136.
6. Bowsher WG, Taylor BA, Hughes LE. Morbidity, mortality and local recurrence following regional node dissection for melanoma. *Br J Surg* 1986;73:906–908.
7. Baas PC, Schraffordt Koops H, Hoekstra HJ, van Bruggen JJ, van der Weele LT, Oldhoff J. Groin dissection in the treatment of lower-extremity melanoma. Short-term and long-term morbidity. *Arch Surg* 1992;127:281–286.
8. Das Gupta TK. Results of treatment of 269 patients with primary cutaneous melanoma: a five-year prospective study. *Arch Surg* 1977;186:201–209.
9. Balch CM, Soong SJ, Murad TM, Ingalls AL, Maddox WA. A multifactorial analysis of melanoma III. Prognostic factors in melanoma patients with lymph node metastases (stage II). *Ann Surg* 1981;193:377–388.
10. Cohen MH, Ketcham AS, Felix EL, et al. Prognostic factors in patients undergoing lymphadenectomy for malignant melanoma. *Ann Surg* 1977;297:627–630.
12. Veronesi U, Adamus J, Bandiera DC, et al. Inefficacy of immediate node dissection in Stage I melanoma of the limbs. *N Engl J Med* 1977;297:627–630.
13. Veronesi U, Adamus J, Bandiera DC, et al. Delayed regional lymph node dissection in Stage I melanoma of the skin of the lower extremities. *Cancer* 1982;49:2420–2430.
14. Sim FH, Taylor WF, Pritchard DJ, Soule EH. Lymphadenectomy in the management of Stage I malignant melanoma: a prospective randomized study. *Mayo Clin Proc* 1986;61:697–705.
15. Balch CM. The role of elective lymph node dissection in melanoma: Rationale, results and controversies. *J Clin Oncol* 1988;6:163–172.
16. Balch CM, Soong SJ, Milton GW, et al. A comparison of prognostic factors and surgical results in 1786 patients with localized (Stage I) melanoma treated in Alabama and New South Wales, Australia. *Ann Surg* 1982;196:677–684.
17. Drepper H, Köhler CO, Bastian B, et al. Benefit of elective lymph node dissection in subgroups of melanoma patients. *Cancer* 1993;72:741–749.
18. Kroon BBR, Jonk A. Elective lymph node dissection in melanoma: still a controversial issue. *Nether J Surg* 1991:43–4:129–132.
19. Morton DL, Wen D-R, Wong JH, et al. Technical details of intraoperative lymphatic mapping for early stage melanoma. *Arch Surg* 1992;127:392–399.
20. Reintgen D, Cruse CW, Wells K, et al. The orderly progression of melanoma nodal metastases. *Ann Surg* 1994;220:759–767.
21. Uren RF, Howman-Giles RB, Shaw HM, Thompson JF, McCarthy WH. Lymphoscintigraphy in high-risk melanoma of the trunk: predicting draining node groups, defining lymphatic channels and locating the sentinel node. *J Nucl Med* 1993;34:1435–1440.
22. Kapteijn BAE, Baidjnath Panday RKL, Liem IH, et al. Lymphoscintigraphy and intraoperative gamma probe detection of the first draining lymph node in clinically localized melanoma. *J Nucl Med* 1995;36:222.
23. Pijpers R, Collet GJ, Meijer S, Hoekstra OS. The impact of dynamic lymphoscintigraphy and gamma probe guidance on sentinel node biopsy in melanoma. *Eur J Nucl Med* 1995;22:1238–1241.
24. Krag DN, Meijer SJ, Weaver DL, et al. Minimal-access surgery for staging of malignant melanoma. *Arch Surg* 1995;130:654–658.
25. Godellas CV, Berman CG, Lyman G, et al. The identification and mapping of melanoma regional nodal metastases: minimally invasive surgery for the diagnosis of nodal metastases. *Am Surgeon* 1995;61:97–101.
26. Essner R, Foshag L, Morton DL. Intraoperative radiolymphoscintigraphy: a useful adjunct to intraoperative lymphatic mapping and selective lymphadenectomy in patients with clinical Stage I melanoma. *Soc Surg Oncol* 1994:104.
27. Das Gupta T, McNeer G. The incidence of metastasis to accessible lymph nodes from melanoma of the trunk and extremities–its therapeutic significance. *Cancer* 1964:897–911.
28. West JH, Seymour JC, Drane WE. Combined transmission-emission imaging in lymphoscintigraphy. *Clin Nucl Med* 1993;18:762–764.
29. Kapteijn BAE, Nieweg OE, Valdés Olmos RA, et al. Reproducibility of lymphoscintigraphy for lymphatic mapping in cutaneous melanoma. *J Nucl Med* 1997;37:972–975.
30. Mudun A, Murray DR, Herda SC, et al. Early stage melanoma: lymphoscintigraphy, reproducibility of sentinel node detection and effectiveness of the intraoperative gamma probe. *Radiology* 1996;199:171–175.
31. Sullivan DC, Croker BP, Harris CC, Deery P, Seigler HF. Lymphoscintigraphy in malignant melanoma: ^{99m}Tc-antimony sulfur colloid. *Am J Radiology* 1981;137:847–851.

32. Alex JC, Weaver DL, Fairbank JT, Rankin BS, Krag DN. Gamma-probe-guided lymph node localization in malignant melanoma. *Surg Oncol* 1993;2:303–308.
33. Hotze A, Mahlstedt J, Wolf F. Radiopharmaceuticals for bone marrow imaging. In: Mahlstedt J, ed. *Bone marrow imaging*. Darmstadt, Germany: GIT Verlag Ernst Giebeler; 1984:5–7.
34. Ciambellotti E, Lanza E, Coda C, Cartia GL. Lymphoscintigraphy: a comparison of two microcolloids labeled with ^{99m}Tc. *Min Med* 1986;77:313–316.
35. Frühling J. Comparative study of four ^{99m}Tc-labeled microcolloids used for lymphoscintigraphy [Abstract]. *Eur J Nucl Med* 1984;9:A43.
36. Lamki LM, Haynie TP, Balch CM, et al. Lymphoscintigraphy in the surgical management of patients with truncal melanoma: comparison of technetium sulfur colloid with technetium human serum albumin [Abstract]. *J Nucl Med* 1989;30:844.

Impact of Lymphoscintigraphy on Sentinel Node Identification with Technetium-99m-Colloidal Albumin in Breast Cancer

Rik Pijpers, Sybren Meijer, Otto S. Hoekstra, Gerard J. Collet, Emile F.I. Comans, Rob P.A. Boom, Paul J. van Diest and Gerrit J.J. Teule

Departments of Nuclear Medicine, Surgical Oncology, Pathology and Surgery, and Academisch Ziekenhuis van de Vrije Universiteit, Amsterdam; Amstelveen Hospital, Amstelveen, The Netherlands

Identification of the sentinel node by using colloidal tracers and a gamma probe or lymphoscintigraphy could be an effective alternative for the complicated original dye-oriented approach. We studied the sentinel node detection rate using early and delayed imaging in breast cancer patients. **Methods:** Thirty-seven patients were imaged 2 hr and 18 hr after peritumoral injection of ^{99m}Tc-colloidal albumin. Preoperatively, axillary foci were located with a handheld gamma probe that was also used to isolate radiolabeled nodes from the axillary dissection specimens. The predictive value of the sentinel node for the axillary tumorstatus was evaluated with histological examination. **Results:** Two and 18 hr after injection, lymphoscintigraphy revealed one to three separate axillary lymph nodes in 33 and 34 patients, respectively. In 30 patients the axillary foci were easily localized with the gamma probe preoperatively. In all 34 patients (92%), with visualized axillary foci, at least one radioactive sample could be retrieved using the gamma probe (total 53 samples). Metastases were found in the sentinel nodes of 11 patients, in seven of 11 being the only tumor-positive lymph node in the axilla. There were no false-negative sentinel nodes. **Conclusion:** The selective targeting and prolonged intranodal retention of ^{99m}Tc-colloidal albumin allows successful sentinel node identification in most (92%) patients.

Key Words: sentinel node; technetium-99m-colloidal albumin; breast cancer; gamma probe; lymphoscintigraphy

J Nucl Med 1997; 38:366–368

In breast cancer, axillary involvement is still the most important prognostic factor on which adjuvant therapy is based (*1*). Staging of the regional lymphatic basin is traditionally performed by axillary lymph node dissection (ALND). Whereas most axillary specimens do not contain metastases (*2*), ALND accounts for more morbidity and costs than the surgical treatment of the primary tumor (*3–5*).

Selective biopsy of the first tumor draining lymph node (sentinel node, SN) may be an alternative for ALND in staging breast cancer patients. The SN concept has been validated in melanoma by intraoperative lymphatic mapping, using vital dye (*6*) or radioactive tracers (*7–9*). A tumor-negative SN virtually excluded lymphatic involvement of the entire regional lymphatic basin.

The concept is now being evaluated in breast cancer. The largest study was performed by Giuliano et al. who used dye-guided lymphatic mapping for SN biopsy. They reported that the SN predicted the axillary tumor status correctly in 96% of the successful biopsies (*10*). However, the method is tedious and, even in experienced hands, meticulous search revealed no SN in 20% of the patients. The apparent extensive learning curve seems to be another obstacle, since surgical breast cancer treatment should remain feasible in daily clinical practice and not just in specialized centers. Attempts are made to simplify SN identification using radioactive colloidal tracers.

Krag et al. described 100% accuracy in 18 patients, using ^{99m}Tc-sulfur colloid and a gamma probe (*11*). This method appears to be considerably easier than the dye approach. However, in this study no SN could be detected in 18% of the patients. It has been suggested that smaller particles like ^{99m}Tc antimony sulfide show faster passage through the lymphatics, and could reduce the number of negative procedures to about 10% (*12*). In an earlier study in melanoma patients with ^{99m}Tc-colloidal albumin we found labeling of SNs in each patient, and an attractive dwell time in the SN (*9*). Kinetic data of colloidal tracers are not available for SN localization in breast cancer. In this study, we determined the SN detection rate using the independent variable of early and delayed imaging followed by gamma probe guided search for the SN in the axillary specimen.

MATERIALS AND METHODS

Thirty-seven consecutive patients (age 58 ± 12 yr) with breast cancer (core biopsy proven) and without clinical evidence of axillary metastases, scheduled for lumpectomy or mastectomy and ALND, were included in the study. The tumor measured <2.0 cm (T1) in 14 patients and 2.0–4.0 cm (T2) in 23, and was located in the following quadrants: upper outer (17 tumors), lower outer (4 tumors), lower inner (3 tumors), upper inner (6 tumors) and central (7 tumors). The day before surgery, 40 MBq ^{99m}Tc-colloidal albumin in 4 ml saline (particle size 3–80 nm; 77 ± 12% <30 nm) was injected in two to four depots in the axillary peritumoral hemisphere. Medial depots were not given as visualization of parasternal drainage does not have clinical consequences presently. Anterior and lateral views (300 sec) were obtained after 2 hr and 18 hr postinjection using a LFOV dual-head gamma camera. Anterior images were obtained both with and without medial shift of the breast. During lateral imaging the arm was abducted at an angle of 180° to minimize attenuation. Images were acquired in a 128 × 128 matrix (16-bit deep pixels) and stored on optical disk. Anatomical landmarks (acromion, jugular notch, xiphoid process) were indicated on the skin with indelible ink and imaged (^{57}Co-

Received Mar. 26, 1996; revision accepted Jul. 15, 1996.
For correspondence or reprints contact: Rik Pijpers, MD, Dept. of Nuclear Medicine, Academisch Ziekenhuis van de Vrije Universiteit, P.O. Box 7057, 1007 MB Amsterdam, The Netherlands.